

Imaging Agents | Hot Paper |

Hyperpolarized ^{129}Xe Magnetic Resonance Imaging Sensor for H_2S Shengjun Yang,^[a] Yaping Yuan,^[a] Weiping Jiang,^[a] Lili Ren,^[a] He Deng,^[a] Louis S. Bouchard,^[b] Xin Zhou,^{*[a]} and Maili Liu^{*[a]}

Abstract: A new magnetic resonance imaging (MRI) molecular sensor for hydrogen sulfide detection and imaging using the nuclear spin resonance of hyperpolarized ^{129}Xe is developed. The designed MRI sensor employs cryptophane for NMR sensing, together with an azide group serving as a reaction site. It demonstrates a “proof-of-concept” that a fluorescent H_2S probe can be linked to a xenon-binding cryptophane and thereby converted into an MRI probe, which could provide a very generalizable template.

Hydrogen sulfide (H_2S), traditionally known for its characteristic offensive odor and toxicity, has recently been shown to be a significant gaseous signaling transmitter in living organisms.^[1] The involvement of endogenous H_2S has been demonstrated in several physiological and pathological processes,^[2] such as regulation of cell growth, cardiovascular protection, modulation of neurotransmission, and anti-inflammation action. Moreover, recent studies have shown that any imbalance H_2S levels can lead to health problems,^[3] including the symptoms of Alzheimer’s disease, Down’s syndrome, and diabetes.

Over the past few decades, several methods have been given to develop H_2S sensors, such as colorimetry,^[4] electrochemical analysis,^[5] and gas chromatography.^[6] Unfortunately, these traditional methods often require complicated post processing and destruction of specimens, and do not provide bio-distributions. Recently, fluorescence detection has developed

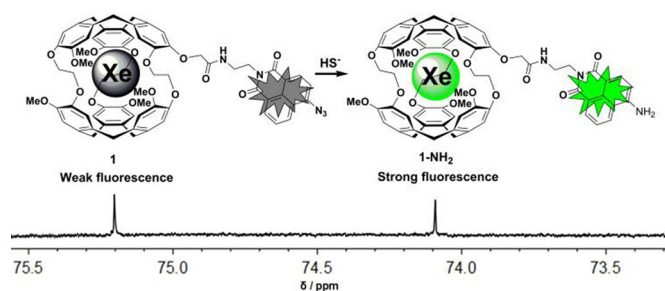
into an attractive approach, because fluorescence probes have been instrumental to elucidate the roles of H_2S in biological systems.^[7] These probes are almost always based on the H_2S -mediated specific reactions, such as reduction reaction, nucleophilic reaction, and metal–sulfide precipitation.^[8] However, the main drawback of poor penetration depth, light scattering in optically opaque media, and associated background noise prevent the use of these fluorescent probes in thick tissues. On the other hand, magnetic resonance imaging (MRI) can generate tomographic images and the penetration depth in tissue is not a limitation. Most MRI sensors developed to date are based on either ^1H or ^{19}F NMR resonances, which relies on modulation of spin relaxation rates or chemical shifts upon binding.^[9] However, these particular resonances have intrinsically low sensitivity and offer poor chemical specificity. Therefore, sensitive MRI methods for specific mapping H_2S distribution are in high demanded to understand its biological role in living systems.

One way for signal enhancement is hyperpolarization and parahydrogen-induced polarization (PHIP) has been used for sensing sulfur-containing compounds.^[10] We propose to enhance the sensitivity with the use of a specific reaction-based hyperpolarized ^{129}Xe MRI sensor. ^{129}Xe nuclei can be hyperpolarized by spin exchange optical pumping (SEOP) to increase the NMR signal by up to four orders of magnitude. In addition, ^{129}Xe has a wide spectral window of more than 200 ppm in biological systems, which renders it highly susceptible to local chemical environment and facilitates the detection of biomolecules or biochemical reactions.^[11] Several biosensors based on hyperpolarized ^{129}Xe have been developed featuring a molecular cage of cryptophane to encapsulate a Xe atom for molecular imaging. Such host molecular systems have been successfully developed for the detection of variety of species, including metal ions,^[12,13] biothiols,^[14] glycans,^[15] proteins,^[16] enzymes,^[17] nucleic acids,^[18] and transmembrane receptor targets,^[19] as well as for use in pH measurements.^[20] The sensitivity of ^{129}Xe magnetic resonance could be further enhanced beyond that achieved by hyperpolarization alone if hyperpolarized ^{129}Xe nuclei are detected using the chemical exchange saturation transfer (Hyper-CEST) method,^[17] in which reversible exchange can be used for indirect detection of caged molecules. This Hyper-CEST technique enables the detection of biomolecules and reactions occurring at much lower concentrations. Recently, biosensing studies involving Hyper-CEST have achieved molecular imaging of living cells.^[15,19a,20a,21] Therefore, sensors based on Hyper-CEST now constitute a potential strategy for molecular imaging in living cellular environments.

[a] Dr. S. Yang, Y. Yuan, W. Jiang, Dr. L. Ren, Dr. H. Deng, Prof. Dr. X. Zhou, Prof. Dr. M. Liu
Key Laboratory of Magnetic Resonance in Biological Systems
State Key Laboratory of Magnetic Resonance and Atomic and Molecular Physics
National Center for Magnetic Resonance in Wuhan
Wuhan Institute of Physics and Mathematics
Chinese Academy of Sciences, Wuhan 430071 (China)
E-mail: xinzhou@wipm.ac.cn
mL.liu@wipm.ac.cn

[b] Prof. Dr. L. S. Bouchard
Department of Chemistry and Biochemistry
California NanoSystems Institute
The Molecular Biology Institute, University of California
Los Angeles, CA 90095 (USA)

Supporting information and the ORCID identification number(s) for the author(s) of this article can be found under:
<http://dx.doi.org/10.1002/chem.201605768>.



Scheme 1. Schematic of ^{129}Xe MRI sensor **1** for H_2S detection and imaging.

Continuing our interest in developing hyperpolarized xenon-based sensors,^[13,14] herein we report a new ^{129}Xe MRI sensor for H_2S detection based on a H_2S -specific response reaction (Scheme 1). To investigate the feasibility of this design concept, we chose cryptophane-A as a host for ^{129}Xe and a known H_2S -mediated specific response group as the reaction site. An azide reduction reaction can selectively detect H_2S , because the azide group can be easily converted into amine upon reaction with H_2S .^[22] The working hypothesis here is that characteristic changes of the azide group lead to chemical structure conversion and finally, signal modulation of the ^{129}Xe NMR chemical shift and also the fluorescence. To test this hypothesis, we coupled the cryptophane derivative to the weakly fluorescent molecule 4-azide-1,8-naphthalic anhydride with ethylenediamine as a tether. The target sensor **1** was readily obtained in few steps from a modified cryptophane-A derivative (used in racemic form) and 4-bromo-1,8-naphthalic anhydride (see Scheme S1 in the Supporting Information). All the synthesized compounds were well characterized by ^1H and ^{13}C NMR spectroscopy, as well as HRMS (see Supporting Information).

With sensor **1** in hand, we firstly investigated its optical property in 20 mM HEPES (4-(2-hydroxyethyl)-1-piperazine-ethanesulfonic acid, pH 7.4) buffer with 60% DMSO as cosolvent at 25 °C. Sodium bisulfide (NaHS) was used as H_2S donor in this study. As designed, sensor **1** was found to be weakly fluorescent (Figure 1) with a major absorption band at 373 nm (see Figure S1 in the Supporting Information). After addition of 10 equivalents of HS^- to the colorless solution of sensor **1**, a rapid change to pale yellow and simultaneously a strong green fluorescence were observed. The UV/Vis spectra show that the maximum absorption peak of sensor **1** exhibited a 62 nm red-shift. Fluorescence spectra show the intensity at 534 nm gradually increased along with the time until it reaches emission saturation (about 25-fold) within 10 min, which was also indicated by kinetic studies of sensor **1** with 10 equivalents of HS^- (see Figure S2). These results suggest that sensor **1** shows fast response towards H_2S .

Encouraged by the above results, the application of sensor **1** in hyperpolarized ^{129}Xe NMR (the level of ^{129}Xe hyperpolarization is about 20%) spectroscopy was evaluated. Under the same test conditions, the ^{129}Xe NMR spectrum of sensor **1** shows two distinct resonances that are assigned to the signal of free xenon in solution calibrated at $\delta = 240.6$ ppm and the signal of encapsulated xenon in sensor **1** at $\delta = 75.2$ ppm. No-

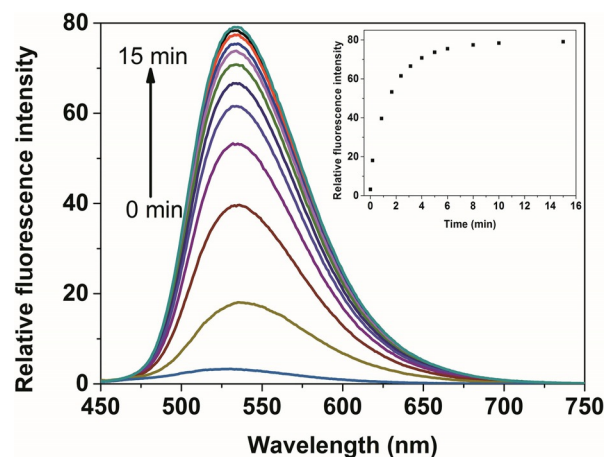


Figure 1. Fluorescence changes of sensor **1** (10 μM) upon addition of 10 equivalents of HS^- in HEPES buffer solution (pH 7.4, 20 mM). Spectra were collected for 0 to 15 min at 25 °C with excitation at 435 nm. The inset shows a time course of the fluorescence intensity change.

tably, a new signal at $\delta = 74.1$ ppm emerges and meanwhile the signal at $\delta = 75.2$ ppm disappears after the addition of 10 equivalents of HS^- . Evidently, a chemical shift change of 1.1 ppm between the signals of caged xenon in the absence and presence of HS^- was observed (Figure 2). These results reveal that the response of sensor **1** towards HS^- leads to a chemical structure transformation that can be detected and differentiated by hyperpolarized ^{129}Xe NMR spectroscopy.

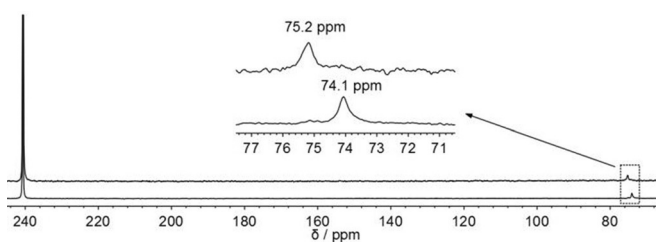


Figure 2. ^{129}Xe NMR spectrum change of sensor **1** (100 μM) upon addition of 10 equivalents of HS^- . The spectra were obtained with two scans under the conditions of 20 mM HEPES (pH 7.4) buffer with 60% DMSO as cosolvent at 25 °C. The inset was the enlarged regional spectra.

The chemical shift changes are likely to be a consequence of an azide reduction reaction induced by HS^- . The azide group is an electron-withdrawing group and can be easily converted to an amino group by electron transfer. This chemical structure conversion alters the electronic density of the NMR moiety, causing a change in the electronic properties of cryptophane, leading to a chemical shift change for the caged xenon. These results clearly demonstrate that ^{129}Xe NMR is extremely sensitive to the chemical environment and can sense the structure transformation of sensor **1** induced by HS^- . Based on the well-established azide reduction mechanism,^[22] the above results can be attributed to the formation of compound **1-NH₂**, which is the product of sensor **1** with HS^- and also confirmed by HRMS experiments (see Figure S3).

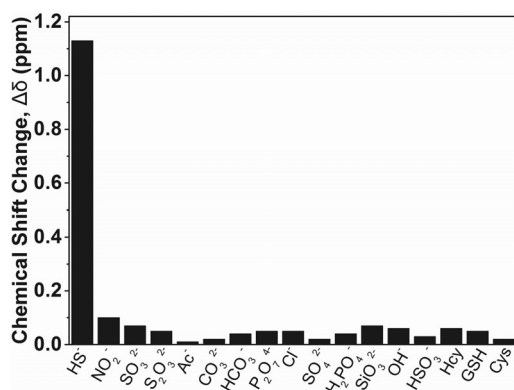


Figure 3. ^{129}Xe NMR chemical shift change of sensor 1 ($100\ \mu\text{M}$) after addition of 10 equivalents of various other species (except for Cys, which is 4 equivalent) for 10 min. Bars represent the value of the ^{129}Xe chemical shift in the presence of various other species relative to the ^{129}Xe chemical shift of sensor 1. All the spectra were obtained with two scans under the conditions of 20 mM HEPES (pH 7.4) buffer with 60% DMSO as cosolvent at $25\ ^\circ\text{C}$.

We then investigated the selectivity of sensor 1 for HS^- against various other species, such as NO_2^- , SO_3^{2-} , $\text{S}_2\text{O}_3^{2-}$, Ac^- , CO_3^{2-} , HCO_3^- , $\text{P}_2\text{O}_7^{4-}$, Cl^- , SO_4^{2-} , H_2PO_4^- , SiO_3^{2-} , OH^- , HSO_3^- , Hcy, GSH, and Cys. As shown in Figure 3, it was found that only the addition of HS^- induced a significant chemical shift change in sensor 1 (see Figure S4). In contrast, addition of other analytes showed almost no significant chemical shift change. These results indicate that sensor 1 exhibits high selectivity for HS^- over other test species by hyperpolarized ^{129}Xe NMR technique. Furthermore, the selectivity of sensor 1 for H_2S was also probed by means of a fluorescence method that also show high selectivity for HS^- (see Figure S5).

Following the observation that sensor 1 exhibits high specificity for H_2S , an attempt was made to investigate the ^{129}Xe MRI properties using a frequency-selective gradient echo sequence to verify the practical applicability in vitro. Such a sequence centered at 74.1 ppm was used to obtain the images of sensor 1 (Figure 4A) without and (Figure 4B) with HS^- . The difference between the two images illustrates that H_2S can be detected and localized by ^{129}Xe MRI.

Finally, we sought to explore the magnetic resonance imaging ability of sensor 1 for H_2S in living cells. The confocal laser scanning microscope was used to image H_2S and localize the sensor due to its high sensitivity and subcellular resolution.

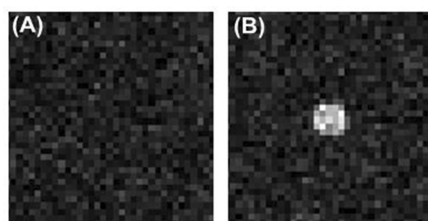


Figure 4. ^{129}Xe axial gradient-echo MRI images of a 10 mm tube containing A) $100\ \mu\text{M}$ sensor 1 and B) $100\ \mu\text{M}$ sensor 1 treated with 10 equivalents of HS^- for 10 min under the test conditions. Images were acquired with a soft radiofrequency pulse centered at $\delta = 74.1\ \text{ppm}$.

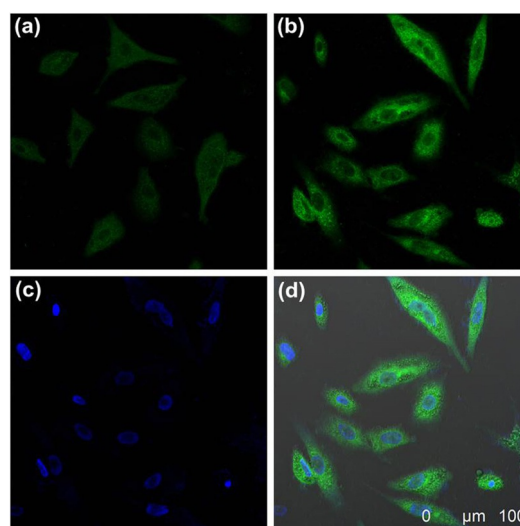


Figure 5. Confocal fluorescence images of HS^- using sensor 1 in A549 cells. a) control experiment, A549 cells incubated with sensor 1 ($10\ \mu\text{M}$) for 2 h; b)–d) NaHS ($100\ \mu\text{M}$) pre-treated (0.5 h) A549 cells incubated with sensor 1 ($10\ \mu\text{M}$) for another 2 h. a),b) Green channel, Emission was collected at 500–650 nm upon excitation at 488 nm. c) Blue channel: nuclear staining (DAPI), Emission was collected at 408–500 nm upon excitation at 405 nm. d) Merged images of b) and c). Scale bar = $100\ \mu\text{m}$.

Strong fluorescence in A549 cells was observed after pretreatment with HS^- ($100\ \mu\text{M}$) for 30 min and further incubation with sensor 1 ($10\ \mu\text{M}$) for another 2 h (Figure 5). As a control, confocal microscope images of A549 cells incubated with sensor 1 ($10\ \mu\text{M}$) in culture medium for 2 h at $37\ ^\circ\text{C}$ showed weak fluorescence. As indicated by the strong intracellular green fluorescence, sensor 1 was found to be rapidly internalized by A549 cells and situated mainly in the cytoplasmic compartments. This result demonstrates that sensor 1 can respond to HS^- through azide reduction reaction in living cells. By way of the fluorescence method, H_2S in living cells assays were originally established and sensor 1 was confirmed to localize in the cytoplasm. We then used hyperpolarized ^{129}Xe NMR to detect H_2S and image the living cells at a concentration of $1 \times 10^7\ \text{cells mL}^{-1}$. As shown in Figure 6a, no significant signal of caged xenon in living cells could be detected after pretreatment with HS^- ($200\ \mu\text{M}$) for 0.5 h and further incubation with sensor 1 ($25\ \mu\text{M}$) for another 2 h through direct acquisition of ^{129}Xe NMR signal (4096 signal averages). On the other hand, the same experiment of caged xenon detection in living cells using the ^{129}Xe Hyper-CEST method in a direct bubbling phantom yielded a Hyper-CEST response centered at around 74.0 ppm (Figure 6b), a characteristic signal of cryptophane-caged xenon. This signal was then used for imaging by using Hyper-CEST MRI (see Figure 6c and Figure S6 in the Supporting Information). However, a Hyper-CEST response of caged xenon in A549 cells at around 74.0 ppm was also detected after incubation with sensor 1 ($25\ \mu\text{M}$) for 2 h (see Figure S7a), while in the blank experiment, no signals were found (see Figure S7b). This result indicates that the chemical shift of sensor 1 without H_2S in A549 cells is almost the same as that of sensor 1 with H_2S . It could be concluded that the chemical shift of sensor 1

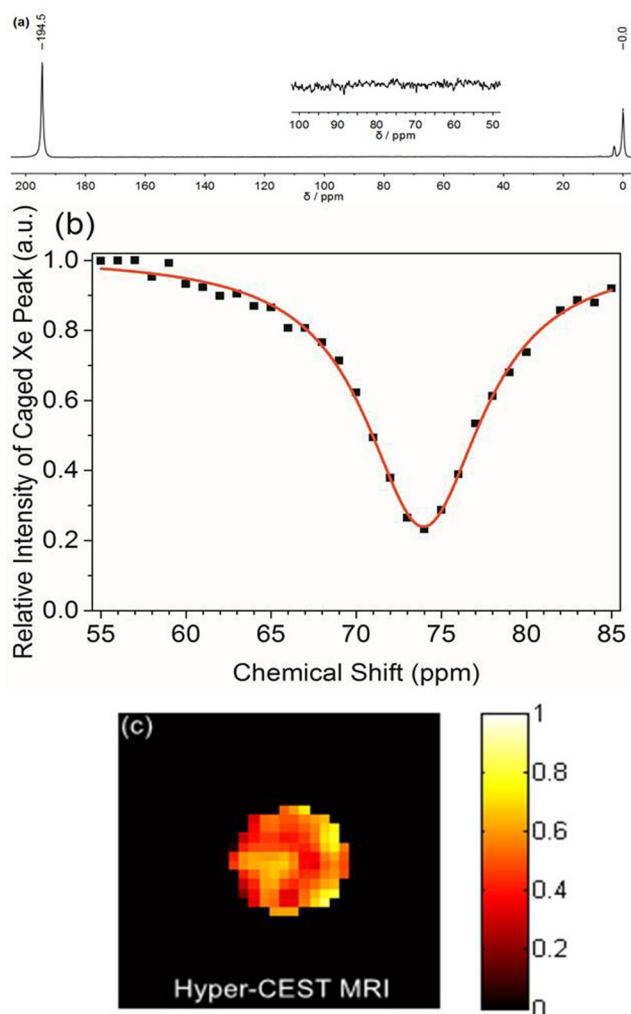


Figure 6. a) ^{129}Xe NMR spectrum of sensor 1 labeled A549 cells (treated with $200\ \mu\text{M}$ NaHS for 0.5 h then incubated with $25\ \mu\text{M}$ sensor 1 for another 2 h) obtained by 4096 signal averages. b) Hyper-CEST spectra of sensor 1 labeled A549 cells (treated with $200\ \mu\text{M}$ NaHS for 0.5 h then incubated with $25\ \mu\text{M}$ sensor 1 for another 2 h). Exponential Lorentzian fits are shown as red solid lines. c) MRI of Hyper-CEST effect. The Hyper-CEST effect was calculated by using the formula $\text{CEST effect} = (\text{offRes} - \text{onRes}) / \text{offRes}$.

with and without H_2S in living cells is hardly differentiated by Hyper-CEST spectrum presently.

In conclusion, we have presented a ^{129}Xe sensor for molecular imaging utilizing hyperpolarized ^{129}Xe nuclear spin resonance. We constructed an azide reduction reaction-based ^{129}Xe sensor, which is composed of modified cryptophane-A derivative to report chemical information through the ^{129}Xe chemical shift. The azide group serves as a reaction site for the H_2S -specific response. This sensor exhibits a chemical shift change of 1.1 ppm (upfield) of caged xenon upon binding to H_2S . The response and cytoplasmic localization in living cells with and without H_2S are well supported by fluorescence and magnetic resonance data. By demonstrating that fluorescent H_2S probe can be converted into an MRI probe by linking to a xenon-binding cryptophane probably offers a universal strategy to analogical sensors.

Acknowledgements

Supports from the Natural Science Foundation of China (81227902, 81625011) and National Program for Support of Eminent Professionals (National Program for Support of Top-notch Young Professionals) are acknowledged.

Conflict of interest

The authors declare no conflict of interest.

Keywords: cryptophane · hydrogen sulfide · hyperpolarization · imaging agents · xenon

- [1] D. Boehning, S. H. Snyder, *Annu. Rev. Neurosci.* **2003**, *26*, 105–131.
- [2] a) H. Kimura, *Exp. Physiol.* **2011**, *96*, 833–835; b) L. Li, P. Rose, P. K. Moore, *Annu. Rev. Pharmacol. Toxicol.* **2011**, *51*, 169–187; c) G. D. Yang, L. Wu, B. Jiang, W. Yang, J. Qi, K. Cao, Q. Meng, A. K. Mustafa, W. Mu, S. Zhang, S. H. Snyder, R. Wang, *Science* **2008**, *322*, 587–590; d) L. Li, M. Bhatia, P. K. Moore, *Curr. Opin. Pharmacol.* **2006**, *6*, 125–129; e) H. Kimura, *Amino Acids* **2011**, *41*, 113–121.
- [3] a) K. Eto, T. Asada, K. Arima, T. Makifuchi, H. Kimura, *Biochem. Biophys. Res. Commun.* **2002**, *293*, 1485–1488; b) W. Yang, G. Yang, X. Jia, L. Wu, R. Wang, *J. Physiol.* **2005**, *569*, 519–531; c) P. Kamoun, M.-C. Belardinelli, A. Chabli, K. Lallouchi, B. Chadeaux-Veke-mans, *Am. J. Med. Genet. A.* **2003**, *116*, 310–311; d) L. Wu, W. Yang, X. Jia, G. Yang, D. Duridanova, K. Cao, R. Wang, *Lab. Invest.* **2009**, *89*, 59–67.
- [4] a) D. Jiménez, R. Martínez-Máñez, F. Sancenón, J. V. Ros-Lis, A. Benito, J. Soto, *J. Am. Chem. Soc.* **2003**, *125*, 9000–9001.
- [5] a) D. G. Searcy, M. A. Peterson, *Anal. Biochem.* **2004**, *324*, 269–275; b) A. Tangerman, *J. Chromatogr. B* **2009**, *877*, 3366–3377.
- [6] a) J. Radford-Knoery, G. A. Cutter, *Anal. Chem.* **1993**, *65*, 976–982; b) R. Hyspler, A. Ticha, M. Indrova, Z. Zadak, L. Hysplerova, J. Gasparic, J. Churacek, *J. Chromatogr. B* **2002**, *770*, 255–259.
- [7] a) F. Yu, X. Han, L. Chen, *Chem. Commun.* **2014**, *50*, 12234–12249; b) V. S. Lin, W. Chen, M. Xian, C. J. Chang, *Chem. Soc. Rev.* **2015**, *44*, 4596–4618; c) C. Zhao, X. Zhang, K. Li, S. Zhu, Z. Guo, L. Zhang, F. Wang, Q. Fei, S. Luo, P. Shi, H. Tian, W.-H. Zhu, *J. Am. Chem. Soc.* **2015**, *137*, 8490–8498; d) W. Xuan, C. Sheng, Y. Cao, W. H. He, W. Wang, *Angew. Chem. Int. Ed.* **2012**, *51*, 2282–2284; *Angew. Chem.* **2012**, *124*, 2328–2330.
- [8] a) J. Chan, S. C. Dodani, C. J. Chang, *Nat. Chem.* **2012**, *4*, 973–984; b) Y. Zhao, T. D. Biggs, M. Xian, *Chem. Commun.* **2014**, *50*, 11788–11805.
- [9] a) S. Viswanathan, Z. Kovacs, K. N. Green, S. J. Ratnakar, A. D. Sherry, *Chem. Rev.* **2010**, *110*, 2960–3018; b) P. Verwilst, S. Park, B. Yoon, J. S. Kim, *Chem. Soc. Rev.* **2015**, *44*, 1791–1806; c) A. D. Sherry, Y. K. Wu, *Curr. Opin. Chem. Biol.* **2013**, *17*, 167–174; d) I. Tirotta, V. Dichiarante, C. Pigiaccielli, G. Cavallo, G. Terraneo, F. B. Bombelli, P. Metrangolo, G. Resnati, *Chem. Rev.* **2015**, *115*, 1106–1129.
- [10] a) R. V. Shchepin, D. A. Barskiy, A. M. Coffey, B. M. Goodson, E. Y. Chekmenev, *ChemistrySelect* **2016**, *1*, 2552–2555; b) O. G. Salnikov, D. B. Burueva, D. A. Barskiy, G. A. Bukhtiyarova, K. V. Kovtunov, I. V. Koptuyug, *ChemCatChem* **2015**, *7*, 3508–3512; c) X. Zhou, D. Graziani, A. Pines, *Proc. Natl. Acad. Sci. USA* **2009**, *106*, 16903–16906; d) P. Berthault, G. Huber, H. Desvaux, *Prog. Nucl. Magn. Reson. Spectrosc.* **2009**, *55*, 35–60.
- [11] C. Dybowski, N. Bansal, T. M. Duncan, *Annu. Rev. Phys. Chem.* **1991**, *42*, 433–464.
- [12] N. Kotera, N. Tassali, E. Léonce, C. Boutin, P. Berthault, T. Brotin, J.-P. Du-tasta, L. Delacour, T. Traoré, D. A. Buisson, F. Taran, S. Coudert, B. Rous-seau, *Angew. Chem. Int. Ed.* **2012**, *51*, 4100–4103; *Angew. Chem.* **2012**, *124*, 4176–4179.
- [13] a) J. Zhang, W. Jiang, Q. Luo, X. Zhang, Q. Guo, M. Liu, X. Zhou, *Talanta* **2014**, *122*, 101–105; b) Q. Guo, Q. Zeng, W. Jiang, X. Zhang, Q. Luo, X. Zhang, L.-S. Bouchard, M. Liu, X. Zhou, *Chem. Eur. J.* **2016**, *22*, 3967–3970.

- [14] a) S. Yang, W. Jiang, L. Ren, Y. Yuan, B. Zhang, Q. Luo, Q. Guo, L.-S. Bouchard, M. Liu, X. Zhou, *Anal. Chem.* **2016**, *88*, 5835–5840; b) Q. Zeng, Q. Guo, Y. Yuan, Y. Yang, B. Zhang, L. Ren, X. Zhang, Q. Luo, M. Liu, L.-S. Bouchard, X. Zhou, *Anal. Chem.* **2017**, *89*, 2288–2295.
- [15] C. Witte, V. Martos, H. M. Rose, S. Reinke, S. Klippel, L. Schröder, C. P. R. Hackenberger, *Angew. Chem. Int. Ed.* **2015**, *54*, 2806–2810; *Angew. Chem.* **2015**, *127*, 2848–2852.
- [16] a) L. Schröder, T. J. Lowery, C. Hilty, D. E. Wemmer, A. Pines, *Science* **2006**, *314*, 446–449; b) M. M. Spence, S. M. Rubin, I. E. Dimitrov, E. J. Ruiz, D. E. Wemmer, A. Pines, S. Q. Yao, F. Tian, P. G. Schultz, *Proc. Natl. Acad. Sci. USA* **2001**, *98*, 10654–10657; c) N. Kotera, E. Dubost, G. Milano, E. Doris, E. Gravel, N. Arhel, T. Brotin, J.-P. Dutasta, J. Cochrane, E. Mari, C. Boutin, E. Léonce, P. Berthault, B. Rousseau, *Chem. Commun.* **2015**, *51*, 11482–11484; d) N. S. Khan, B. A. Riggle, G. K. Seward, Y. Bai, I. J. Dmochowski, *Bioconjugate Chem.* **2015**, *26*, 101–109.
- [17] a) Q. Wei, G. K. Seward, P. A. Hill, B. Patton, I. E. Dimitrov, N. N. Kuzma, I. J. Dmochowski, *J. Am. Chem. Soc.* **2006**, *128*, 13274–13283; b) J. A. Aaron, J. M. Chambers, K. M. Jude, L. Di Costanzo, I. J. Dmochowski, D. W. Christianson, *J. Am. Chem. Soc.* **2008**, *130*, 6942–6943; c) J. M. Chambers, P. A. Hill, J. A. Aaron, Z. Han, D. W. Christianson, N. N. Kuzma, I. J. Dmochowski, *J. Am. Chem. Soc.* **2009**, *131*, 563–569; d) S. Korchak, W. Kilian, L. Schröder, L. Mitschang, *J. Magn. Reson.* **2016**, *265*, 139–145.
- [18] V. Roy, T. Brotin, J.-P. Dutasta, M. H. Charles, T. Delair, F. Mallet, G. Huber, H. Desvaux, Y. Boulard, P. Berthault, *ChemPhysChem* **2007**, *8*, 2082–2085.
- [19] a) C. Boutin, A. Stopin, F. Lenda, T. Brotin, J.-P. Dutasta, N. Jamin, A. Sanson, Y. Boulard, F. Letaurtre, G. Huber, A. B. Buchmann, N. Tassali, H. Desvaux, M. Carrière, P. Berthault, *Bioorg. Med. Chem.* **2011**, *19*, 4135–4143; b) H. M. Rose, C. Witte, F. Rossella, S. Klippel, C. Freund, L. Schröder, *Proc. Natl. Acad. Sci. USA* **2014**, *111*, 11697–11702; c) F. Rossella, H. M. Rose, C. Witte, J. Jayapaul, L. Schröder, *ChemPlusChem* **2014**, *79*, 1463–1471.
- [20] a) B. A. Riggle, Y. Wang, I. J. Dmochowski, *J. Am. Chem. Soc.* **2015**, *137*, 5542–5548; b) L. Schröder, L. Chavez, T. Meldrum, M. Smith, T. J. Lowery, D. E. Wemmer, A. Pines, *Angew. Chem. Int. Ed.* **2008**, *47*, 4316–4320; *Angew. Chem.* **2008**, *120*, 4388–4392; c) P. Berthault, H. Desvaux, T. Wendlinger, M. Gyejacquot, A. Stopin, T. Brotin, J.-P. Dutasta, Y. Boulard, *Chem. Eur. J.* **2010**, *16*, 12941–12946.
- [21] a) K. K. Palaniappan, R. M. Ramirez, V. S. Bajaj, D. E. Wemmer, A. Pines, M. B. Francis, *Angew. Chem. Int. Ed.* **2013**, *52*, 4849–4853; *Angew. Chem.* **2013**, *125*, 4949–4953; b) S. Klippel, J. Döpfert, J. Jayapaul, M. Kunth, F. Rossella, M. Schnurr, C. Witte, C. Freund, L. Schröder, *Angew. Chem. Int. Ed.* **2014**, *53*, 493–496; *Angew. Chem.* **2014**, *126*, 503–506; c) M. Schnurr, J. Sloniec-Myszk, J. Döpfert, L. Schröder, A. Hennig, *Angew. Chem. Int. Ed.* **2015**, *54*, 13444–13447; *Angew. Chem.* **2015**, *127*, 13645–13648; d) G. K. Seward, Y. Bai, N. S. Khan, I. J. Dmochowski, *Chem. Sci.* **2011**, *2*, 1103–1110.
- [22] a) Z.-J. Chen, H.-W. Ai, *Biochemistry* **2014**, *53*, 5966–5974; b) S. K. Bae, C. H. Heo, D. J. Choi, D. Sen, E.-H. Joe, B. R. Cho, H. M. Kim, *J. Am. Chem. Soc.* **2013**, *135*, 9915–9923; c) J. Cao, R. Lopez, J. M. Thacker, J. Y. Moon, C. Jiang, S. N. S. Morris, J. H. Bauer, P. Tao, R. P. Mason, A. R. Lippert, *Chem. Sci.* **2015**, *6*, 1979–1985; d) V. S. Lin, A. R. Lippert, C. J. Chang, *Proc. Natl. Acad. Sci. USA* **2013**, *110*, 7131–7135.

Manuscript received: December 11, 2016
 Revised manuscript received: February 21, 2017
 Accepted manuscript online: February 28, 2017
 Version of record online: March 21, 2017